

Double-type-I charge-injection heterostructure for quantum-dot light-emitting diodes

Li-Xi WANG,^{1,2‡} Cindy G. TANG,^{1‡} Zhao-Siu TAN,³ Hao-Yu PHUA,¹ Jing CHEN,² Wei LEI,² Rui-Qi PNG^{1*}, Lay-Lay CHUA,^{1,3*} Peter K.H. HO¹

¹ Department of Physics, National University of Singapore, Lower Kent Ridge Road, S117550, Singapore

² Joint International Research Laboratory of Information Display and Visualization, School of Electronic Science and Engineering, Southeast University, Nanjing, People's Republic of China

³ Department of Chemistry, National University of Singapore, Lower Kent Ridge Road, S117552, Singapore

* Correspondence to:

R.Q.P. (ruiqi@nus.edu.sg) or L.L.C. (chmcll@nus.edu.sg)

‡ These authors contributed equally to the work.

Supplementary Information

Contents

1. Supplementary Figures	2
2. Supplementary Table	7

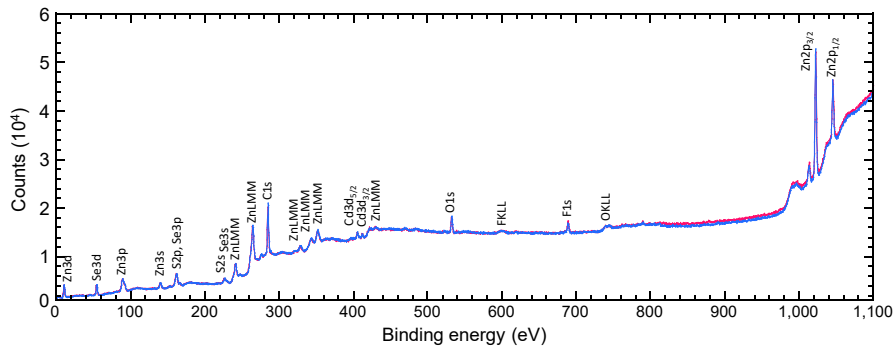


Fig. S1 X-ray photoemission analysis of Mesolight® blue-emitting QDs. 20-nm-thick film was spin-cast on Si/Au/25-nm PEDT:PSSH substrate, and annealed to 100°C on a digital hotplate for 5 min in a nitrogen glovebox, and transferred under nitrogen to XPS load lock. Excitation, MgK α . Duplicate samples, red data after a long ultraviolet photoemission spectroscopy run (50 min). Constant analyzer energy, 50 eV.

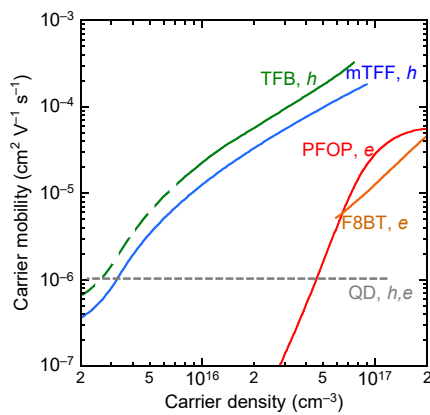


Fig. S2 Carrier mobility of polymer semiconductors. Legend: *e*, electron; *h*, hole. Carrier mobility was extracted using Mott–Gurney equation from experimental current–voltage characteristics of 80–140-nm-thick spin-cast semiconductor films fitted with Ohmic contact for the desired carrier sign, and plotted against average carrier density in the film. Grey dashed line, assumed effective hole mobility of QD layer ($1 \times 10^{-6} \text{ cm}^2 \text{ V}^{-1} \text{ s}^{-1}$). Electron mobility is even smaller ($1 \times 10^{-6} \text{ cm}^2 \text{ V}^{-1} \text{ s}^{-1}$) and can be neglected, as suggested in the literature.

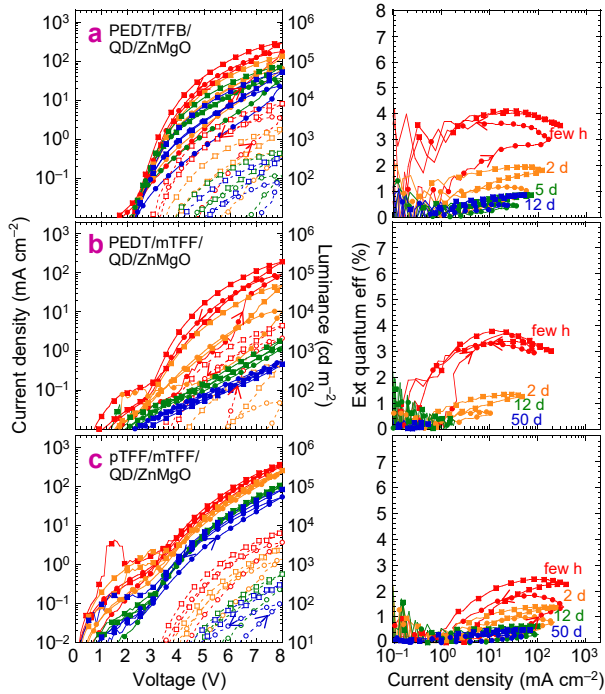


Fig. S3 Blue-QLED characteristics for ZnMgO as electron injection layer. Current density–voltage–luminance JVL (**left**), and external quantum efficiency η – J (**right**) of: **(a)** ITO/30nm PEDT:PSSH/35nm TFB/20nm blue-QD/60nm ZnMgO/Al, **(b)** ITO/30nm PEDT:PSSH/35nm mTFF/20nm blue-QD/60nm ZnMgO/Al, **(c)** ITO/10nm pTFF-C₂F₅SIS/35nm mTFF/20nm blue-QD/60nm ZnMgO/Al. pTFF-C₂F₅SIS is hole doped. JVL plots: solid line, closed symbols (J), dashed line, open symbols (L); red (freshly made devices), blue (after storage). Every five data point shown. Two representative diodes shown in their second voltage sweep. Sweep protocol: 0 to +8 V then to –3 and back to 0 V.

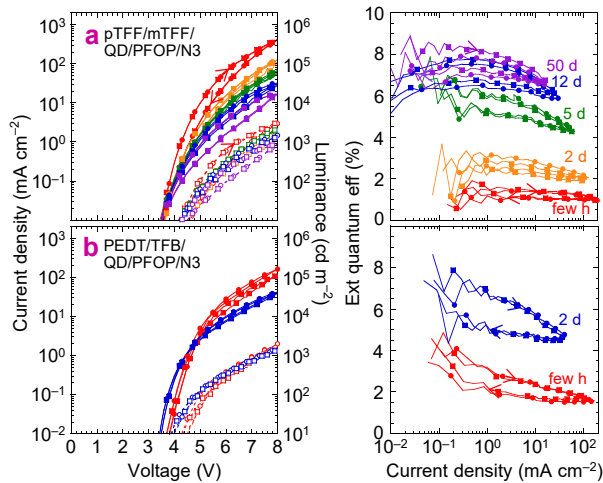


Fig. S4 Blue-QLED characteristics of hole-injection stacks with different hole-injection efficiency for same Al/N3/PFOP electron-injection stack. Current density–voltage–luminance JVL (**left**), and external quantum efficiency η – J (**right**) of: **(a)** ITO/10nm pTFF- C_2F_5SIS /35nm mTFF/20nm blue-QD/60nm PFOP/20nm N3(Ox,AcO)/Al, **(b)** ITO/30nm PEDT:PSSH/35nm TFB/20nm blue-QD/60nm PFOP/20nm N3(Ox,AcO)/Al. pTFF- C_2F_5SIS is hole doped, N3 is electron doped. JVL plots: solid line, closed symbols (J), dashed line, open symbols (L); red (freshly made devices), blue (after storage). Every five data point shown. Two representative diodes shown in their second voltage sweep. Sweep protocol: 0 to +8 V then to –3 and back to 0 V.

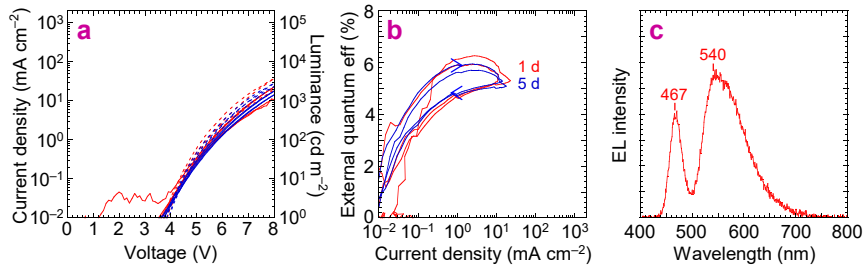


Fig. S5 White QLED with ZnMgO/F8BT as electron-injection stack. (a) Current density–voltage–luminance *JVL* characteristics, (b) external quantum efficiency η – J characteristics, and (c) uncorrected electroluminescence spectrum. Diode structure: ITO/10nm hole-doped pTFF-C₂F₅SIS/35nm mTFF/20nm blue-QD/10nm F8BT/50nm ZnMgO/Al. *JVL* plots: red lines and blue lines, J , after elapsed time; corresponding dashed lines, L . Two representative diodes shown. Scan protocol: 0 to +8 V then to –3 and back to 0 V.

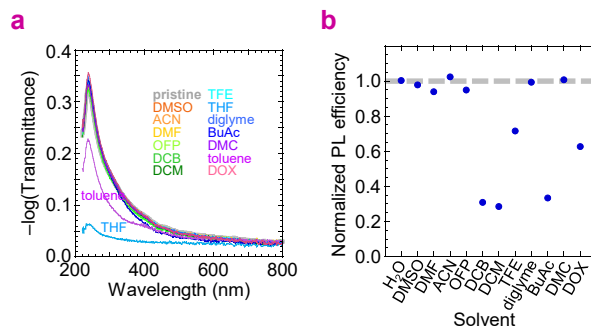


Fig. S6 Solvent compatibility of the blue-QDs. (a) Transmission optical spectra and (b) Photoluminescence (PL) of QD films collected before and after contacting with different solvents. PL excitation wavelength is 365-nm. PL was normalized to the PL of pristine films. DMSO is dimethyl sulfoxide; ACN, acetonitrile; DMF, *N,N*-dimethylformamide; OFP, 2,2,3,3,4,4,5,5-octafluoro-1-pentanol; DCB, *o*-dichlorobenzene, DCM dichloromethane; TFE, 2,2,2-trifluoroethanol; THF, tetrahydrofuran; BuAc, butyl acetate; DMC, dimethyl carbonate; DOX, 1,4-dioxane. Experimental protocol: 30-nm blue-QD film was first spin-cast on oxygen-plasma-cleaned fused silica substrates, contacted with solvent for 5 s on spinner, then spun dry.

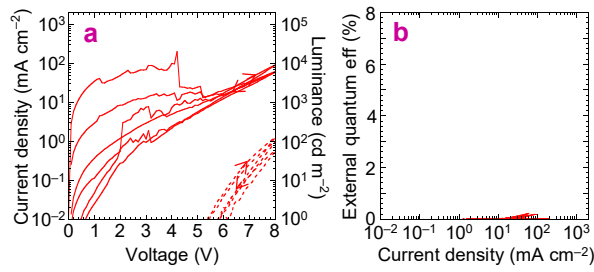


Fig. S7 Device with TSPO1 ETL. Device structure: ITO/30nm PEDT:PSSH/35nm mTFF/20nm blue-QD/35nm TSPO1/50nm ZnMgO/Al. TSPO1 is diphenyl(4-(triphenylsilyl)phenyl)phosphine oxide and is spin-cast from OFP solution. **(a)** Current density–voltage–luminance JVL characteristics, and **(b)** external quantum efficiency η – J characteristics. JVL plots: red lines, J ; corresponding dashed lines, L . Three representative diodes shown. Scan protocol: 0 to +8 V then to -3 and back to 0 V.

Table S1. Dielectric constant and refractive index

SN	Material	Dielectric constant and refractive index ^a	
		ϵ_r	n_{470}
1	QD emitter layer	3.0	1.55
2	Polymer HTL	3.0	1.75
3	Polymer ETL	3.0	1.77
4	Polymer HIL	∞	1.3–0.2i
5	Polymer EIL	∞	1.77–0.01i
6	ZnO nanoparticle layer	∞	2.1
7	ITO	∞	2.01–0.04i
8	Glass	7.8	1.53
9	Al	∞	0.67–5.69i
10	Pd	∞	1.58–3.58i
11	Ag	∞	0.14–2.64i

^a Dielectric constant (ϵ_r) and refractive index at 470 nm (n_{470}). The values for polymers were measured by spectroscopic ellipsometry. The values for QD emitter layer and ZnO nanoparticle layer were computed from bulk values by Bruggeman effective medium theory for close-packed spherical particle films. Both ϵ_r and n_{470} are strongly decreased by the void spaces between particles, and for QDs, further by the organic ligand-coating. The values for other materials were taken from literature. ϵ_r is ∞ for electrically conducting materials.